Journal of The Electrochemical Society, **154** (9) H773-H777 (2007)
0013-4651/2007/154(9)/H773/5/$20.00 © The Electrochemical Society

Improvement of the Morphological Stability by Stacking RuO_2 on Ru Thin Films with Atomic Layer Deposition

Se-Hun Kwon,[a] Oh-Kyum Kwon,[b] Jae-Hoon Kim,[b] Seong-Jun Jeong,[a] Sung-Wook Kim,[a] and Sang-Won Kang[a,z]

[a]*Department of Materials Science and Engineering, Korea Advanced Institute of Science and Technology, Yusong-gu, Taejon 305-701, Korea*
[b]*Samsung Electronics Company, Limited, Semiconductor Business, Giheung-Eup Yongin-City, Gyeonggi-Do, Korea*

Stacked RuO_2/Ru structures were produced by atomic layer deposition (ALD) using an alternating supply of bis(ethylcyclopentadienyl)ruthenium [$Ru(EtCp)_2$] and O_2 gas at a deposition temperature of 270°C. The type of the deposited film, either Ru or RuO_2, was controlled by the total pressure in the ALD system as well as the ratio of the adsorbed $Ru(EtCp)_2$ to the partial pressure of O_2 in the following O_2 gas pulse. The resistivity of the deposited Ru and RuO_2 thin films was about 15 and 70 $\mu\Omega$ cm, respectively. The surface morphology of Ru films annealed in O_2 ambient was seriously degraded by surface oxidation. Moreover, RuO_2 films were also agglomerated due to the residual stress releasing during the annealing process. However, a stacked RuO_2/Ru structure produced using ALD maintained a smooth surface even at an annealing temperature of 800°C in ambient O_2. Auger electron spectroscopy confirmed that the stacked RuO_2/Ru structure successfully blocked oxygen and silicon diffusion. Therefore, the stacked RuO_2/Ru structure produced by ALD is suitable for use as the bottom electrode material for high dielectric applications.
© 2007 The Electrochemical Society. [DOI: 10.1149/1.2750448] All rights reserved.

Manuscript submitted February 12, 2007; revised manuscript received April 26, 2007. Available electronically July 6, 2007.

High dielectric materials, such as TiO_2, Ta_2O_5, and $(Ba,Sr)TiO_3$, have been studied for application in storage capacitors for next-generation dynamic random access memory (DRAM).[1-4] For this application to be successful, the choice of a suitable material for the bottom electrode is very important. The electrode should not react with oxygen (O) or silicon (Si). It should also prevent diffusion in either direction between the dielectric layer and the underlying poly-Si plug.[5,6] Moreover, a compatible etching process, good morphological stability, and reliable adhesion properties are necessary when applying such materials in electronic devices. Ru is one of the promising electrode materials for use in high dielectric capacitors, because it can block the diffusion of O during the fabrication and annealing of dielectrics by forming conductive oxide films, RuO_2.[7,8] In addition, Ru has a relatively low resistivity (7.1 $\mu\Omega$ cm) and dry etching of the thin film is easily accomplished using reactive ion etching.

Despite being fabricated with dielectrics of high permittivity, the capacitor in Gbit-scale DRAMs requires a three-dimensional structure to provide sufficient storage capacitance. Therefore, to construct capacitor electrodes of Ru or RuO_2 thin film, an atomic layer deposition (ALD) technique that provides excellent conformality is necessary. The ALD process has many inherent advantages over conventional physical vapor deposition or chemical vapor deposition techniques, including good conformality, accurate thickness controllability, uniformity over large areas, and high film qualities at low growth temperatures.[9] In our previous paper, we reported an ALD technique for growing Ru and RuO_2 thin films using an alternating supply of bis(ethylcyclopentadienyl)ruthenium [$Ru(EtCp)_2$] and O_2 gas,[10] where the control of the deposited film, either Ru or RuO_2, is determined by the relative ratio of the $Ru(EtCp)_2$ adsorbed on the film surface to the partial pressure of O_2 in the following O_2 pulse. However, it was found that the Ru or RuO_2 film prepared by ALD cannot be used alone as the bottom electrode for high dielectric films because both Ru and RuO_2 films were vulnerable to severe post heat treatment. Here, we present further results, including the control of the deposited film, either Ru or RuO_2, as well as the fabrication of nanoscale stacked structure of RuO_2/Ru thin film using this characteristic of the ALD system with $Ru(EtCp)_2$ and O_2 gas. The stacked RuO_2/Ru structure was not affected by severe annealing conditions, and it effectively blocked the diffusion of O and Si, indicating that the stacked RuO_2/Ru structure is suitable for use as a bottom electrode.

Experimental

Ru and RuO_2 thin films were deposited on Si(100) and SiO_2 (100 nm)/Si substrates at a deposition temperature of 270°C using an alternating supply of [$Ru(EtCp)_2$] and O_2 gas. Before deposition, the Si(100) substrates were cleaned in a HF solution and rinsed in deionized water to remove the native oxide. $Ru(EtCp)_2$ is a liquid precursor with good thermal stability and a relatively high vapor pressure of 0.18 Torr at 80°C. $Ru(EtCp)_2$ was contained in a bubbler, which was heated to 80°C, and carried by Ar gas at a flow rate of 50 sccm. To prevent precursor condensation in the feed line, the stainless steel delivery line was heated to 90°C. One deposition cycle of Ru and RuO_2 ALD consisted of four steps: (*i*) an exposure of the $Ru(EtCp)_2$ precursor, (*ii*) a purge pulse with 50 sccm Ar, (*iii*) an exposure of O_2 gas mixed with Ar, and (*iv*) another purge with 50 sccm Ar. This cycle was repeated as many times as necessary to obtain the desired film thickness. During the O_2 pulse, O_2 gas was introduced at rates from 20 to 120 sccm mixed with 100 sccm Ar. The thickness of deposited films was analyzed using field emission scanning electron microscopy. The film resistivity was calculated from the sheet resistance measured using a four-point probe and the film thickness. X-ray diffraction (XRD) analysis was used to determine the crystal structure of the deposited films. The film composition and impurities were measured using Rutherford backscattering and elastic recoil detection time-of-flight spectroscopy. To evaluate the O diffusion barrier properties of fabricated thin films, rapid thermal annealing experiments were performed with three kinds of samples (Ru, RuO_2, and a stacked RuO_2/Ru layer) at several temperatures under ambient O_2 and Ar. Before and after annealing, surface morphology changes were estimated using scanning electron microscopy (SEM) and atomic force microscopy (AFM) and O diffusion barrier properties were evaluated using Auger electron spectroscopy (AES) depth analysis.

Results and Discussion

The type of the deposited film, either Ru or RuO_2, was controlled by the $Ru(EtCp)_2$ pulse time and the oxygen partial pressure in the oxygen pulse based on our previous result for Ru ALD on a TiN substrate.[10] Figure 1 shows the resistivity dependence of the deposited film on the $O_2/(Ar + O_2)$ ratio in the O_2 gas pulse under a

[z] E-mail: swkang@kaist.ac.kr

Downloaded on 2016-09-16 to IP 130.203.136.75 address. Redistribution subject to ECS terms of use (see ecsdl.org/site/terms_use) unless CC License in place (see abstract).

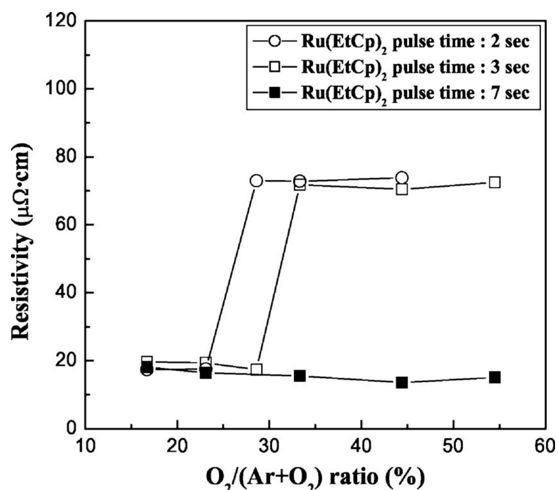

Figure 1. The dependence of the film resistivity on the $O_2/(Ar + O_2)$ ratio in the O_2 gas pulse for a $Ru(EtCp)_2$ pulse time of 2, 3, or 7 s at a total pressure of 1 Torr. To measure the film resistivities, the films were deposited on SiO_2/Si substrate.

pressure of 1 Torr. The O_2 gas pulse time was fixed at 10 s, and the $Ru(EtCp)_2$ pulse time was set at 2, 3, or 7 s, respectively. For a $Ru(EtCp)_2$ pulse time of 7 s, the film resistivity was about 15 μΩ cm regardless of the $O_2/(Ar + O_2)$ ratio. However, for a $Ru(EtCp)_2$ pulse time of 2 or 3 s, the film resistivity increased sharply to about 70 μΩ cm depending on the $O_2/(Ar + O_2)$ ratio. The change in the film resistivity occurred at an $O_2/(Ar + O_2)$ ratio of around 25 and 33%, respectively. From the XRD analysis, it has been confirmed that this sudden change in the film resistivity at a particular $O_2/(Ar + O_2)$ ratio was due to the phase change of the deposited film from Ru to RuO_2, as shown in Fig. 2. The film with a resistivity of about 15 μΩ cm shows the typical XRD pattern of metallic Ru, while that with a resistivity of about 70 μΩ cm indicates RuO_2. However, when the $Ru(EtCp)_2$ pulse time was 7 s, only Ru film was deposited for all $O_2/(Ar + O_2)$ ratios used in this experiment. This was probably because the required $O_2/(Ar + O_2)$ ratio for the conversion from Ru to RuO_2 exceeded 55% for a $Ru(EtCp)_2$ pulse time of 7 s.

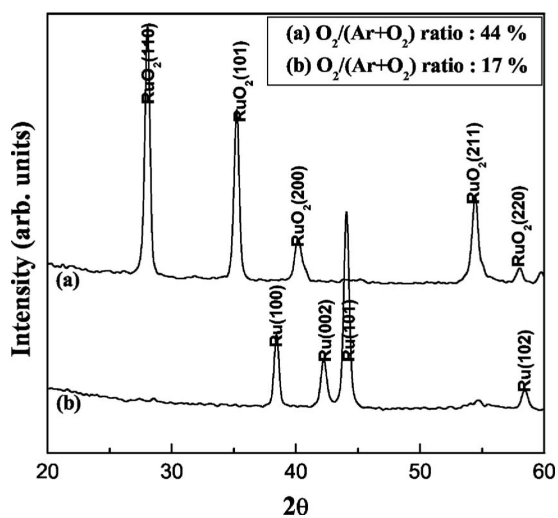

Figure 2. The XRD spectra obtained from films deposited on SiO_2/Si substrate at $O_2/(Ar + O_2)$ ratios of 17 and 44% for a $Ru(EtCp)_2$ pulse time of 2 s.

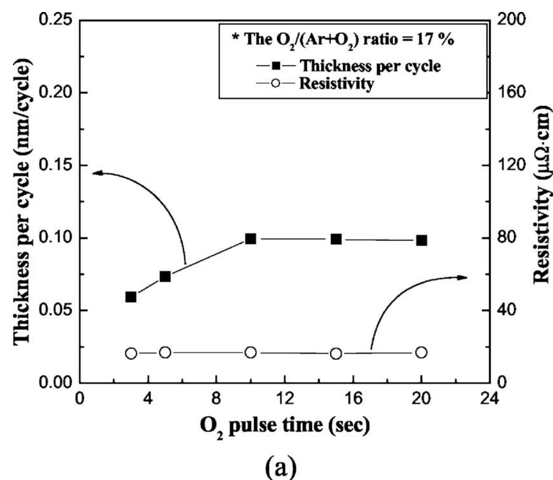

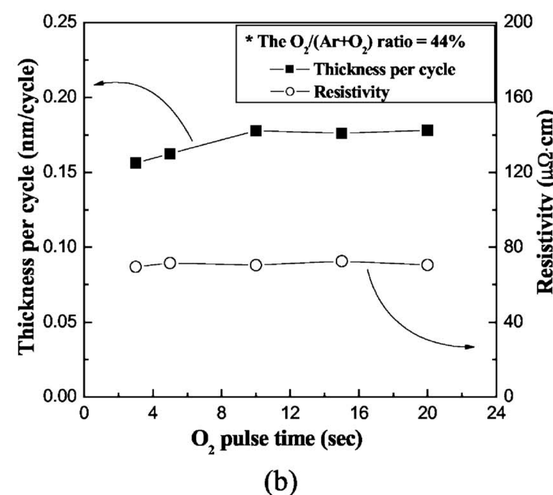

Figure 3. The dependence of both the deposited film thickness per cycle and the resistivity on the oxygen gas pulse time of (a) Ru and (b) RuO_2. The films were deposited on SiO_2/Si substrate. During the deposition of Ru and RuO_2, the $Ru(EtCp)_2$ pulse time was fixed at 3 s. The $O_2/(Ar + O_2)$ ratio was fixed at 17% for Ru and 44% for RuO_2, respectively.

Figure 3 shows the film thickness deposited in one cycle and the resistivity of the deposited film as a function of the O_2 pulse time. The oxygen pulse time was varied from 3 to 20 s, while the $Ru(EtCp)_2$ pulse time was fixed at 3 s. With the $O_2/(Ar + O_2)$ ratio fixed at 17%, only Ru film with a resistivity of about 15 μΩ cm was deposited regardless of the O_2 pulse time, and the deposition rate of Ru was saturated at about 0.10 nm/cycle when the O_2 pulse time exceeded 10 s, as shown in Fig. 3a. However, when the $O_2/(Ar + O_2)$ ratio was fixed at 44%, the deposited film was obviously RuO_2 regardless of the O_2 pulse time. Under the same conditions, the saturated deposition rate of RuO_2 was about 0.17 nm/cycle when the O_2 pulse time exceeded 10 s, as shown in Fig. 3b. Therefore, when the $O_2/(Ar + O_2)$ ratio is fixed at a certain value, the type of the deposited film, either Ru or RuO_2, is independent of the total O_2 dose (O_2 pulse time).

To evaluate the effect of the process pressure, the dependence of the deposited film thickness/cycle and the resistivity on the pressure were investigated. During deposition, the $O_2/(Ar + O_2)$ ratio in the O_2 pulse was set at 55% and $Ru(EtCp)_2$ pulse time was fixed at 7 s. When the process pressure exceeded 3 Torr, the resistivity of the deposited film increased sharply from 15 to 70 μΩ cm, indicating that the deposited film had changed from Ru to RuO_2, as shown in Fig. 4. Since one atomic monolayer of RuO_2 is almost 2.3 times

Downloaded on 2016-09-16 to IP 130.203.136.75 address. Redistribution subject to ECS terms of use (see ecsdl.org/site/terms_use) unless CC License in place (see abstract).

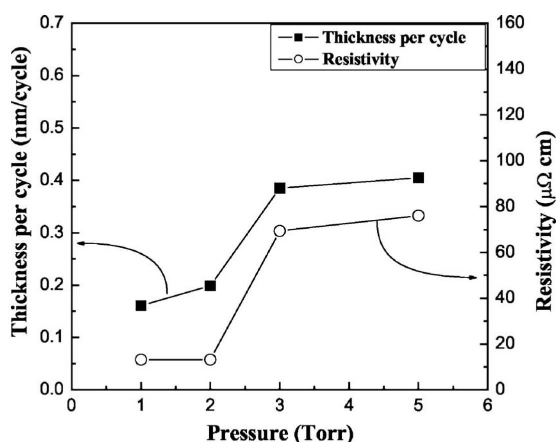

Figure 4. The dependence of both the deposited film thickness per cycle and the resistivity on total pressure at an $O_2/(Ar + O_2)$ ratio of 55%. The films were deposited on SiO_2/Si substrate. During deposition, $Ru(EtCp)_2$ for 7 s and O_2 gas mixed with 100 sccm Ar for 10 s were alternatively supplied.

thicker than an atomic monolayer of Ru, the film thickness/cycle also increased. However, the film thickness/cycle actually obtained at 3 Torr was more than 2.3 times that obtained at 1 Torr, as shown in Fig. 4. This was probably due to the increase in the amount of adsorbed Ru precursor in the $Ru(EtCp)_2$ pulse with the total pressure. Based on these results, we concluded that the type of the deposited film, either Ru or RuO_2, depends on the ratio of the number of Ru precursor molecules adsorbed on the film surface to the O_2 partial pressure supplied during the subsequent O_2 gas pulse. It also depends on the total pressure. Therefore, the film deposition (Ru or RuO_2) can be digitally controlled by changing the process conditions, including the $Ru(EtCp)_2$ pulse time, $O_2/(Ar + O_2)$ ratio in the O_2 gas pulse, and total pressure in the ALD system using $Ru(EtCp)_2$ and O_2 gas. This characteristic of ALD systems using $Ru(EtCp)_2$ and O_2 should be of great benefit in the convenient fabrication of nanoscale stacked structures of RuO_2/Ru thin films.

A smooth surface is one of the requirements for the thin films used as the bottom electrodes of DRAM capacitors, and it must retain during the subsequent deposition and post heat treatment of the dielectrics. Therefore, the surface of Ru and RuO_2 thin films deposited on Si(100) substrates by ALD was investigated using both SEM and AFM before and after annealing under various conditions.

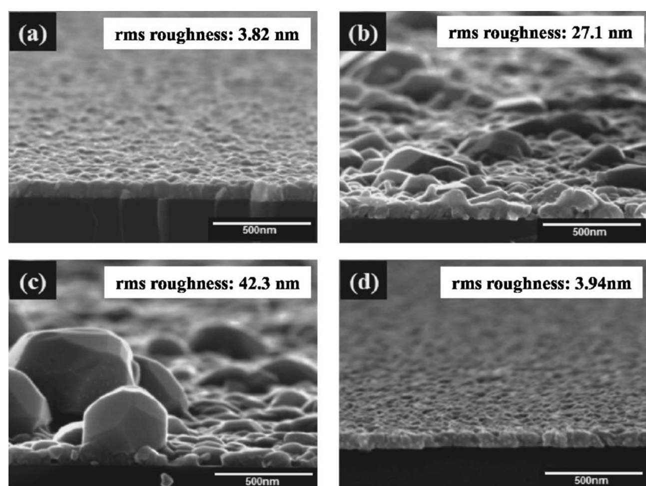

Figure 5. The SEM images and corresponding rms surface roughness values of Ru films deposited on Si substrate: (a) as deposited, (b) annealed at 600°C for 30 min in ambient O_2, (c) annealed at 750°C for 5 min in ambient O_2, and (d) annealed at 750°C for 5 min in ambient Ar.

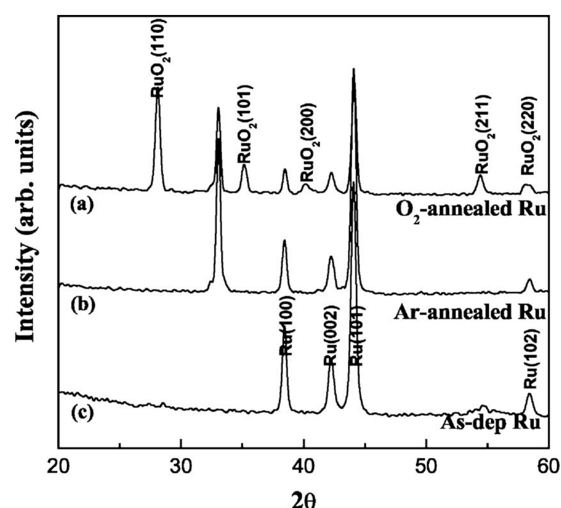

Figure 6. The XRD patterns of Ru films deposited on Si substrate: (a) O_2-annealed Ru film, (b) Ar-annealed Ru film, and (c) as-deposited Ru film.

Figure 5 shows SEM images and the corresponding root mean square (rms) surface roughness values of 80 nm thick Ru films: (a) as-deposited, (b) annealed in ambient O_2 at 600°C for 30 min, (c) annealed in ambient O_2 at 750°C for 5 min, and (d) annealed in ambient Ar at 750°C for 5 min. The rms surface roughness values of these samples were measured using AFM. As shown in Fig. 5b, the surface of the Ru film annealed in ambient O_2 at 600°C for 30 min was worse than the as-deposited Ru film. Moreover, the surface of the Ru film annealed in O_2 atmosphere at 750°C for 5 min was much rougher. However, unlike the O_2-annealed Ru film, the Ar-annealed Ru film surface was not degraded, as shown in Fig. 5d. To clarify the dependence of the morphological change on the annealing conditions, XRD analysis was performed on the annealed Ru films. Figure 6 shows the XRD patterns of films annealed in ambient Ar and O_2, respectively. The Ar-annealed Ru film exhibits the typical XRD pattern generated from Ru metal. The XRD pattern taken from the O_2-annealed Ru film has RuO_2 peaks as well as Ru peaks; this indicates that the surface oxidation during the O_2 annealing process caused surface roughening of the Ru films. Since the deposition and post treatment of high dielectric material requires heating beyond 600°C in an O_2 atmosphere, this means that Ru films alone cannot be used as the bottom electrode for high dielectric films.

Figure 7 shows SEM images and the corresponding rms surface roughness values of 90 nm thick RuO_2 films deposited on Si substrates: (a) as deposited, (b) O_2 annealed at 600°C for 30 min, (c) O_2 annealed at 750°C for 5 min, and (d) Ar annealed at 750°C for 5 min. When RuO_2 film was annealed at 600°C for 30 min in O_2, its surface was slightly roughened, but it is comparable to the as-deposited RuO_2. However, the RuO_2 film became much rougher when annealed in ambient O_2 at 750°C for 5 min, as shown in Fig. 7c. The surface of the Ar-annealed RuO_2 film was also rough, as shown in Fig. 7d. These surface morphology changes were due mainly to agglomeration; i.e., since RuO_2 films on Si substrates are under residual stress, agglomeration during the annealing process releases the stress. The stress of RuO_2 films can be determined from the shift in the XRD spectra of $RuO_2(110)$, since this shift in the XRD spectra is proportional to the lattice distortion of the film. To clarify this residual stress in the RuO_2 films, thin RuO_2 films (200 Å) were deposited on Si substrates. Figure 8 shows the XRD patterns obtained from these films: (a) as deposited, and (b) annealed at 750°C for 5 min in ambient of Ar. According to Joint Committee on Powder Diffraction Standards No. 43-1027, the standard peak position for $RuO_2(110)$ spectra is 28.018°. Figure 8a shows the $RuO_2(110)$ peak at 27.64° in the as-deposited film. This shift indicates that as-deposited RuO_2 films on Si substrates were

Downloaded on 2016-09-16 to IP 130.203.136.75 address. Redistribution subject to ECS terms of use (see ecsdl.org/site/terms_use) unless CC License in place (see abstract).

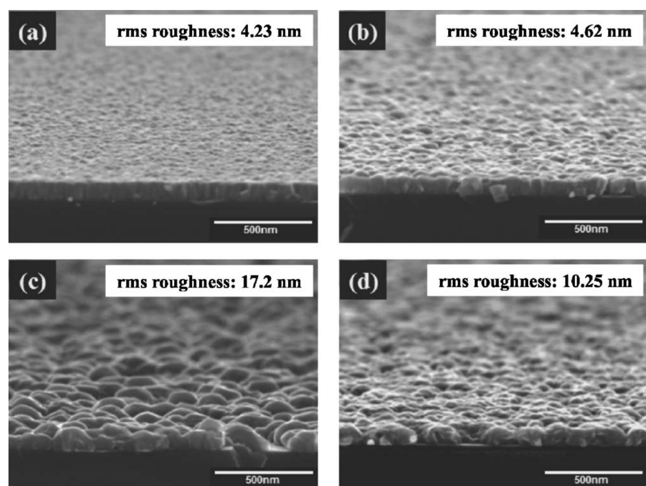

Figure 7. The SEM images and corresponding rms surface roughness values of RuO_2 films deposited on Si substrate: (a) as-deposited, (b) O_2 annealed at 600°C for 30 min, (c) O_2 annealed at 750°C for 5 min, and (d) Ar annealed at 750°C for 5 min.

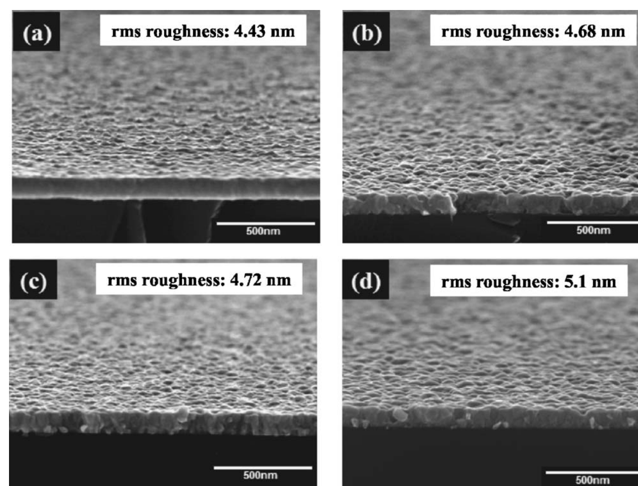

Figure 9. The SEM images and corresponding rms surface roughness values of RuO_2/Ru stack structure prepared on Si substrate: (a) as deposited, (b) annealed at 600°C for 30 min, (c) annealed at 750°C for 5 min, and (d) annealed at 800°C for 5 min in ambient O_2.

under tensile residual stress. However, Fig. 8b shows that the peak position for $RuO_2(110)$ is shifted to 27.97° after annealing at 750°C for 5 min in ambient Ar. This spectrum change indicates that residual stress is considerably relieved by the annealing process. From these results, we concluded that the agglomeration of RuO_2 films is due to the release of residual stress during the annealing process, and that single-layered RuO_2 films are also unsuitable as the bottom electrode for high dielectric films.

Therefore, we proposed that a stacked RuO_2/Ru structure can be used as the bottom electrode for high dielectrics. In the stacked RuO_2/Ru structure, the RuO_2 layer can withstand chemical attack in an O_2 atmosphere. The Ru layer may act as a buffer layer to reduce the stress generated between the RuO_2 film and the Si substrate during film deposition.

To investigate surface morphological changes and O diffusion barrier properties, the RuO_2/Ru stack structure was deposited. In this stacked structure, the thicknesses of RuO_2 and Ru were 70 and 40 nm, respectively. Figure 9 shows the SEM images and the corresponding rms surface roughness values of this stack structure: (a) as deposited, (b) annealed at 600°C for 30 min, (c) annealed at 750°C for 5 min, and (d) annealed at 800°C for 5 min in ambient O_2. As expected, the stacked RuO_2/Ru structure on Si maintained a smooth surface even under more severe annealing conditions at 800°C for 5 min in ambient O_2, as shown in Fig. 9.

The O and Si diffusion barrier property of the stacked RuO_2/Ru structure was estimated using AES analysis. Figure 10 shows the

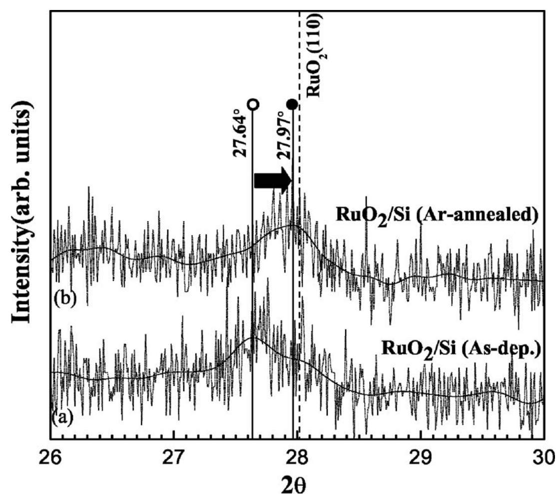

Figure 8. The XRD patterns of RuO_2 films deposited on Si substrate: (a) as deposited, and (b) annealed at 750°C for 5 min in ambient Ar.

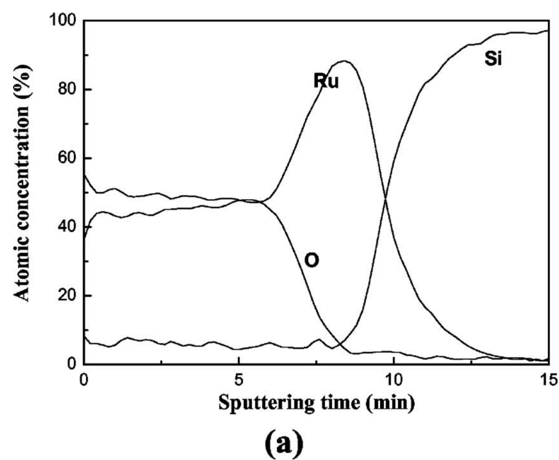

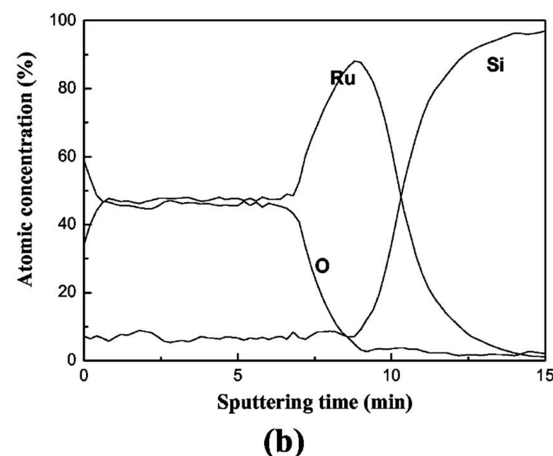

Figure 10. The AES depth profiles of the stacked RuO_2/Ru structures prepared on Si substrate: (a) as deposited and (b) annealed at 800°C for 5 min in ambient O_2.

Downloaded on 2016-09-16 to IP 130.203.136.75 address. Redistribution subject to ECS terms of use (see ecsdl.org/site/terms_use) unless CC License in place (see abstract).

AES depth profiles of the structure RuO_2/Ru stack on Si: (a) as-deposited, and (b) annealed at 800°C for 5 min in ambient O_2. The AES depth profiles indicate that the stacked RuO_2/Ru structure successfully acted as a barrier blocking the inward diffusion of O and the outward diffusion of Si. Since the stacked RuO_2/Ru structure deposited by ALD successfully blocked both O and Si diffusion, and its surface morphology was not affected under severe annealing conditions, RuO_2/Ru stacked layers can serve as the bottom electrode in high dielectric applications.

Conclusions

The ratio of the adsorbed Ru precursor to the O_2 partial pressure in the following O_2 gas pulse determined whether a Ru or RuO_2 film was produced in the ALD system using $Ru(EtCp)_2$ and O_2 gas. Utilizing this characteristic, stacked RuO_2/Ru structures were successfully deposited by ALD at 270°C. The resistivities of Ru and RuO_2 were about 15 and about 70 $\mu\Omega$ cm, respectively. The surface of Ru films annealed in an O_2 atmosphere was seriously degraded by oxidation. Moreover, the RuO_2 film was also roughened by residual stress. However, the stacked RuO_2/Ru structure deposited by ALD remained smooth, even at a high annealing temperature of 800°C in ambient O_2, and successfully blocked both O and Si diffusion. Therefore, the stacked RuO_2/Ru structure deposited by ALD is suitable for use as a bottom electrode material in high dielectric applications.

Acknowledgments

This work was supported by Korea Research Foundation Grant Funded by the Korean Government_MOEHRD_KRF-2005-005-J09702.

Korea Advanced Institute of Science and Technology assisted in meeting the publication costs of this article.

References

1. J. Lin, N. Masaaki, A. Tsukune, and M. Yamada, *Appl. Phys. Lett.*, **74**, 2370 (1999).
2. T. Kawahara, M. Yamamuka, A. Yuuki, and K. Ono, *Jpn. J. Appl. Phys., Part 1*, **35**, 4880 (1996).
3. G. W. Dietz, W. Antpöhler, M. Klee, and R. Waser, *J. Appl. Phys.*, **78**, 6113 (1995).
4. S. G. Yoon and A. Safari, *Thin Solid Films*, **254**, 211 (1995).
5. J. G. Lee, Y. T. Kim, S. Min, and S. H. Choh, *J. Appl. Phys.*, **77**, 5473 (1995).
6. R. Ramesh, *Thin Film Ferroelectric Materials and Devices*, Kluwer Academic Press, Dordrecht, (1997).
7. M. L. Green, M. E. Gross, L. E. Paga, K. J. Schnoes, and D. Brasen, *J. Electrochem. Soc.*, **132**, 2677 (1985).
8. S. Saito and K. Kuramasu, *Jpn. J. Appl. Phys., Part 1*, **31**, 135 (1992).
9. M. Ritala, *Appl. Surf. Sci.*, **112**, 223 (1997).
10. O. K. Kwon, J. H. Kim, H. S. Park, and S. W. Kang, *J. Electrochem. Soc.*, **151**, G109 (2004).

Downloaded on 2016-09-16 to IP 130.203.136.75 address. Redistribution subject to ECS terms of use (see ecsdl.org/site/terms_use) unless CC License in place (see abstract).